Optics & Spectroscopy, 2004, 97 (1): 100-106

Numerical Simulation of Coherent Effects under Conditions of Multiple Scattering

V. L. Kuz'min* and I. V. Meglinski**

** St. Petersburg Institute of Commerce and Economics, St. Petersburg, 194021 Russia*

*** Cranfild University, School of Engineering, Cranfild, MK43OAL, UK*

E-mail: i.meglinski@cranfield.ac.uk

Abstract—The time correlation function and the interference component of the coherent backscattering from a multiple-scattering medium are calculated in the framework of the Monte Carlo technique. By comparing the stochastic Monte Carlo technique with the iteration procedure of solving the Bethe–Salpeter equation, it is shown that the simulation of the optical path of photon packets that have experienced *n* scattering events is exactly equivalent to calculating the *n*th-order ladder diagram. Using this equivalence, the Monte Carlo technique is generalized for simulation of the time correlation functions and coherent backscattering.

1. INTR ODUCTION

Statistical numerical simulation based on the Monte Carlo technique is widely used in studies of propagation of optical radiation in randomly inhomogeneous turbid media [1]. The Monte Carlo methods developed in the framework of solving these particular problems are mainly aimed at calculation of the scattered light intensity. In recent years, considerable attention has focused on the effects related to laser light coherence [2–9]. Coherence is one of the most important parameters of laser light. It characterizes the temporal and spatial stability and quality of the light wavefront. In spite of the strong multiple scattering typical of most randomly inhomogeneous media, coherent effects still noticeably reveal themselves, e.g., in the form of enhanced backscattering, spatiotemporal fluctuations of the light intensity, etc. Numerical simulation of effects of this kind requires a special approach.

The theory of radiation transfer in randomly inhomogeneous and strongly scattering media, including the description of coherent and interference effects, has been successfully developed in the framework of the transfer or Bethe–Salpeter equations [10]. In this paper, by comparing the well-known stochastic Monte Carlo technique with the theoretical approach based on representation of the solution of the Bethe–Salpeter equation as a series expansion in the scattering multiplicities, we show how this technique can be generalized within a united method on passing from numerical calculation of the intensity to calculation of time correlations of the intensity, coherent backscattering, and other coherent effects. We consider here the most popular case in theoretical studies, that of scattering of optical radiation in a medium occupying a half-space with a plane interface. For clarity of description of the method, we consider normal incidence of the light beam.

The structure of this paper is as follows. In the second section, we describe the Monte Carlo technique as applied to the calculation of the intensity of multiply scattered light. In the third section, we consider the method of calculation of the time correlation function of the field and the interference component of the backscattering in the framework of the Bethe–Salpeter equation. The fourth section contains a comparative analysis of the Monte Carlo technique and solution of the Bethe–Salpeter equation. In the fifth section, we present the results of modeling of the time correlation functions and the coherent backscattering peak. In the conclusion, we discuss the results.

2. CALCULATION OF THE INTENSITY OF SCATTERED LIGHT USING THE MONTE CARLO TECHNIQUE

Numerical simulation of the light propagation in a randomly inhomogeneous strongly scattering medium using the Monte Carlo technique is performed in stages. The distance passed by a photon packet between successive scattering events is a random quantity that takes on a value from zero to infinity. The main assumption of the method is that the distribution law has the form [11]

$$f(s) = \mu \exp(-\mu s), \quad (1)$$

where $f(s)$ is the density of the probability that the random quantity s (the free path length) takes on a value within the interval $[s, s + ds]$, $\mu = 1/l$ is the extinction coefficient, l is the extinction length or the mean free path length of the photon packet, and $l = \bar{s}$. Thus, the

dependence of the scattering on particular properties of the medium—namely, the concentration and size of scatterers and the difference in the refractive indices of the scatterers and the medium—is contained, in an integral way, in a single parameter of the distribution function, the mean free path length l.

The light losses are related to the processes of elastic and inelastic collisions of the photons with the matter:

$$\mu = \mu_s + \mu_a, \tag{2}$$

where $\mu_s = 1/l_s$ is the elastic scattering coefficient and $\mu_a = 1/l_a$ is the coefficient of intrinsic absorption; l_s and l_a are, respectively, the scattering and absorption lengths.

It follows from the distribution law (1) that the quantity

$$\xi = \int_s^\infty f(s')ds' \tag{3}$$

is the cumulative probability that the free path length exceeds a specified value s. At the same time, expression (3) makes it possible to find the inverse dependence and to express the random quantity s in terms of the probability ξ. By calculating the integral (3) for a specified distribution (1), we have

$$s = -\frac{\ln\xi}{\mu}. \tag{4}$$

This procedure is one of the key elements of the Monte Carlo technique, which consists in choosing an arbitrary value of ξ using a random number generator within the interval [0, 1].

The change in the direction of motion of the photon packet in each event of elastic scattering is determined by the indicatrix, or the scattering phase function,

$$p(\mathbf{k}_i - \mathbf{k}_s) = \sigma(\mathbf{q})/\int d\Omega_s \sigma(\mathbf{q}), \tag{5}$$

where $\mathbf{k}_i$ and $\mathbf{k}_s$ are the wave vectors, respectively, before and after the scattering; $|\mathbf{q}| = |\mathbf{k}_i - \mathbf{k}_s| = 2k\sin\theta_s/2$ determines the change of the wave vector; θ_s is the angle of scattering with respect to the direction $\mathbf{k}_i$; $\int d\Omega_s$ denotes integration over all possible orientations of the wave vector $\mathbf{k}_s$; and $\sigma(\mathbf{q})$ is the differential scattering cross section at the angle θ_s ($\cos\theta_s = (\mathbf{k}_i, \mathbf{k}_s)k_i^{-2}$. Accordingly, the portion of the light scattered into an elementary solid angle $d\Omega_s$ is $p(\mathbf{k}_i - \mathbf{k}_s)d\Omega_s$.

The random walk trajectory of the photon packet along the path from the source ($\mathbf{r}_S$) to the detector ($\mathbf{r}_D$) is shown schematically in Fig. 1. The value of the detected signal is determined by accumulating statistics over the trajectories as the total weight of all the photon packets reaching the photodetector. The problems related to the reflection on the interface, discussed in detail in [12], are outside the scope of the present paper.

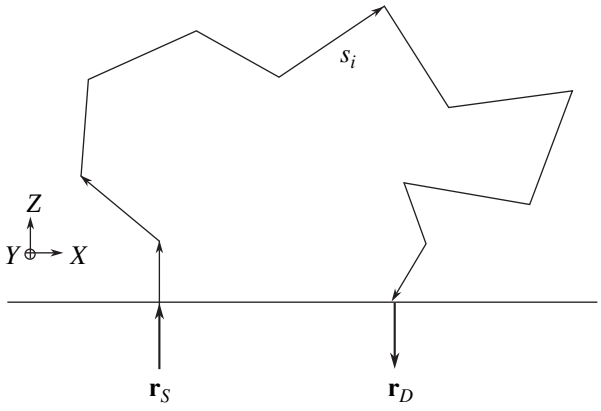


Fig. 1. The trajectory of a photon wandering in a random semi-infinite medium: *S*, light source; *D*, photon detector; s_i, free path length between the $(i-1)$th and ith scattering events.

Now, we will compare the scheme of numerical simulation presented above with the theoretical description of the light propagation in the framework of the Bethe–Salpeter equation.

3. THE BETHE–SALPETER EQUATION

The radiation transfer in a strongly inhomogeneous medium with random spatiotemporal fluctuations of the permittivity is described by the Bethe–Salpeter integral equation,

$$\Gamma(\mathbf{R}_2, \mathbf{R}_1, t|\mathbf{k}_s, \mathbf{k}_i) = k_0^4\tilde{G}(\mathbf{k}_s - \mathbf{k}_i, t)\delta(\mathbf{R}_2 - \mathbf{R}_1) + k_0^4\int d\mathbf{R}_3\tilde{G}(-\mathbf{k}_s + \mathbf{k}_{23}, t)\Lambda(R_{23})\Gamma(\mathbf{R}_3, \mathbf{R}_1, t|\mathbf{k}_{23}, \mathbf{k}_i). \tag{6}$$

Here, $\Gamma(\mathbf{R}_2, \mathbf{R}_1, t|\mathbf{k}_s, \mathbf{k}_i)$ is the Green's function, or propagator, of the Bethe–Salpeter equation, which describes propagation of a pair of complex-conjugate fields, shifted in time by the interval t, from point $\mathbf{R}_1$ to point $\mathbf{R}_2$; the fields arrive at the point $\mathbf{R}_1$ with the wave vector $\mathbf{k}_i$ and emerge from point $\mathbf{R}_2$ with the wave vector $\mathbf{k}_s$, $k_0 = 2\pi/\lambda$ is the wave number; λ is the wavelength; $k_s = k_i = k = nk_0$; n is the refractive index of the medium: $n = n_1 + in_2$, where n_1 and n_2 are, respectively, the real and imaginary parts of n; and $(2n_2k_0)^{-1} = l$. The function $\Lambda(R) = R^{-2}\exp(-R/l)$ is the product of a complex-conjugate pair of the Green's functions of the corresponding wave equation and describes the light propagation between two scattering events. The quantity $\tilde{G}(\mathbf{q}, t)$ is the Fourier transform of the pair correlation function of the permittivity fluctuations $\delta\varepsilon$, responsible for the scattering:

$$\tilde{G}(\mathbf{q}, t) = \frac{1}{(4\pi)^2}\int d\mathbf{r}\langle\delta\varepsilon(0, 0)\delta\varepsilon(\mathbf{r}, t)\rangle\exp(-i\mathbf{qr}). \tag{7}$$

At $t = 0$, the quantity $\tilde{G}(\mathbf{q}, 0)$, to within a constant factor, coincides with the differential cross section of single scattering.

The optical theorem connects the scattering length with the single-scattering cross section integrated over the angles. In the Born approximation, this theorem may be written as [13]

$$1/l_s = k_0^4 \int \tilde{G}(\mathbf{k}_i - \mathbf{k}_s, 0) d\Omega_s. \quad (8)$$

The phase function $p(\mathbf{k}_i - \mathbf{k}_s)$ has the form

$$p(\mathbf{k}_i - \mathbf{k}_s) = \tilde{G}(\mathbf{k}_i - \mathbf{k}_s, 0) / \int \tilde{G}(\mathbf{k}_i - \mathbf{k}_s, 0) d\Omega_s. \quad (9)$$

By analogy with Eq. (9), let us define the quantity

$$p_t(\mathbf{k}_i - \mathbf{k}_s) = \tilde{G}(\mathbf{k}_i - \mathbf{k}_s, t) / \int \tilde{G}(\mathbf{k}_i - \mathbf{k}_s, 0) d\Omega_s. \quad (10)$$

At $t = 0$, this function coincides with the phase scattering function:

$$p_0(\mathbf{k}_i - \mathbf{k}_s) = p(\mathbf{k}_i - \mathbf{k}_s).$$

With allowance for the optical theorem and definition (10), let us represent the Bethe–Salpeter equation in the form

$$\Gamma(\mathbf{R}_2, \mathbf{R}_1, t|\mathbf{k}_s, \mathbf{k}_i) = \mu_s p_t(\mathbf{k}_i - \mathbf{k}_s)\delta(\mathbf{R}_2 - \mathbf{R}_1) + \mu_s \int p_t(\mathbf{k}_{23} - \mathbf{k}_s)\Lambda(R_{23})\Gamma(\mathbf{R}_3, \mathbf{R}_1, t|\mathbf{k}_{31}, \mathbf{k}_i) d\mathbf{R}_3. \quad (11)$$

The Bethe–Salpeter propagator $\Gamma(\mathbf{R}_2, \mathbf{R}_1, t|\mathbf{k}_s, \mathbf{k}_i)$ allows one to calculate the intensity and binary field–field correlations. Here, as usual, it is assumed that, in a strongly inhomogeneous medium, the polarization properties of the electromagnetic field are lost in the process of multiple scattering and one can restrict oneself to consideration of the scalar wave equation.

Equation (6) is written in the weak-scattering approximation ($\lambda \ll l$), which is also referred to as the ladder approximation because it formally arises after summation of a series in the scattering multiplicities as a sum of ladder diagrams.

The main contribution to the scattered light is made by the ladder diagrams. Physically, they describe two successive chains of the scattering processes, the same for both fields $\mathbf{E}(\mathbf{r}, 0)$ and $\mathbf{E}^*(\mathbf{r}, t)$. In view of the identity of these two successions of the scattering, the phase relations between the fields do not change, and the ladder diagrams thus describe the incoherent component. For scattering angles close to 180°, the interference component, related to the cyclic or fan-shaped diagrams, becomes comparable with the main ladder component.

For the experimental geometry, with the scattered light observed at a large distance from the scattering medium, the time correlation function of the field may be represented as the sum

$$C_E(t|\mathbf{k}_s, \mathbf{k}_i) = C^{(L)}(t|\mathbf{k}_s, \mathbf{k}_i) + C^{(V)}(t|\mathbf{k}_s, \mathbf{k}_i), \quad (12)$$

where $C^{(L)}$ and $C^{(V)}$ are the incoherent and interference components of the scattered light (for directions $\mathbf{k}_i$ and $\mathbf{k}_s$ close to the normal one).

Let the scattering medium occupy the half-space $z > 0$, where z is the Cartesian coordinate normal to the boundary of the medium. In this case, the main (ladder) and interference (fan-shaped) components of the coherence function, respectively, have the form

$$C^{(L)}(t|\mathbf{k}_s, \mathbf{k}_i) = \int d\mathbf{R}_1 d\mathbf{R}_2 \Gamma(\mathbf{R}_2, \mathbf{R}_1, t|\mathbf{k}_s, \mathbf{k}_i) \times \exp(-z_1/l\cos\theta_i - z_2/l\cos\theta_s), \quad (13)$$

$$C^{(V)}(t|\mathbf{k}_s, \mathbf{k}_i) = \int d\mathbf{R}_1 d\mathbf{R}_2 \times [\Gamma(\mathbf{R}_2, \mathbf{R}_1, t|(\mathbf{k}_s - \mathbf{k}_i)/2, (\mathbf{k}_i - \mathbf{k}_s)/2) - k_0^4 \tilde{G}(\mathbf{k}_s - \mathbf{k}_i, t)\delta(\mathbf{R}_2 - \mathbf{R}_1)] \times \exp\left[-\frac{z_1 + z_2}{2l}(1/\cos\theta_i + 1/\cos\theta_s) + in_1 k_0 (z_1 - z_2)(\cos\theta_i - \cos\theta_s) + in_1 k_0 (x_1 - x_2)(\sin\theta_i - \sin\theta_s)\right], \quad (14)$$

where θ_i is the angle of incidence and θ_s is the angle of scattering measured from the backscattering direction. The incident and scattered beams lie in the (x, z) plane.

The first term on the right-hand side of Eq. (11) describes the single scattering in the propagator of the Bethe–Salpeter equation. Since the single scattering does not contribute to the interference component of the backscattering, this term is subtracted in the integrand of Eq. (14). For the case of strictly backscattered light, with $\mathbf{k}_s = -\mathbf{k}_i$, the interference component $C^{(V)}(t|\mathbf{k}_s, \mathbf{k}_i)$ coincides exactly with the main, incoherent, component $C^{(L)}(t|\mathbf{k}_s, \mathbf{k}_i)$ before subtraction of the single-scattering contribution.

When simulating such a geometry using the Monte Carlo technique, one should fix the directions of the incident and emerging photon packets at the points $\mathbf{r}_S$ and $\mathbf{r}_D$ lying on the surface of the medium. After that, the summation is performed over all positions $\mathbf{r}_D$.

At $t = 0$, Eq. (13) describes the intensity of the scattered light. Accordingly, Eq. (14) determines the peak of the coherent backscattering. The time correlation function of the intensity is a quadratic form of the correlation function of the field:

$$C_I(t|\mathbf{k}_s, \mathbf{k}_i) = |C_E(t|\mathbf{k}_s, \mathbf{k}_i)|^2. \quad (15)$$

For the experimental geometry with the point source and photodetector located at the surface of the medium at the points $\mathbf{R}_S$ and $\mathbf{R}_D$, respectively, the correlation function of the field is calculated by the formula

$$C_E(\mathbf{R}_D, \mathbf{R}_S, t) = \int \Lambda(\mathbf{R}_D - \mathbf{R}_2) \times \Gamma(\mathbf{R}_2, \mathbf{R}_1, t|\mathbf{k}_{D2}, \mathbf{k}_{1S}) \Lambda(\mathbf{R}_1 - \mathbf{R}_2) d\mathbf{R}_2 d\mathbf{R}_2. \quad (16)$$

Such an experimental geometry can be modeled in a standard way: the points $\mathbf{R}_S$ and $\mathbf{R}_D$ are fixed, while the directions $\mathbf{k}_{D2}$ and $\mathbf{k}_{1S}$, as well as the distances $\mathbf{R}_2$ and $\mathbf{R}_1$, are selected in a random way.

By iterating the Bethe–Salpeter equation, we obtain the series

$$\begin{aligned}\Gamma(\mathbf{R}_2, \mathbf{R}_1, t|\mathbf{k}_s, \mathbf{k}_i) &= \mu_s p(\mathbf{k}_i - \mathbf{k}_s)\delta(\mathbf{R}_2 - \mathbf{R}_1) \\ &+ \mu_s^2 p_t(\mathbf{k}_s - \mathbf{k}_{21})\Lambda(R_{21}) p_t(\mathbf{k}_{21} - \mathbf{k}_i) \\ &+ \mu_s^3 p_t(\mathbf{k}_s - \mathbf{k}_{23})\Lambda(R_{23}) p_t(\mathbf{k}_{23} - \mathbf{k}_{31}) \\ &\times \Lambda(R_{31}) p_t(\mathbf{k}_{31} - \mathbf{k}_i) + \ldots,\end{aligned} \quad (17)$$

usually illustrated by a series of ladder diagrams (Fig. 2).

Physically, series (17) is the expansion in the scattering multiplicities. In fact, it is exactly the summation of such a diagrammatic series, as an operator geometric progression, that leads to the Bethe–Salpeter equation.

4. COMPARATIVE ANALYSIS OF THE MONTE CARLO TECHNIQUE AND THE SERIES IN THE SCATTERING MULTIPLICITIES

Let us compare the method of analytical summation of iteration series (17) with the Monte Carlo technique for the stationary case using, as an example, calculation of the scattered light intensity ($t = 0$) in the absence of absorption ($l = l_s$). Note that the first term on the right-hand side of Eq. (17) describes a single scattering event; the second term, two scattering events; and so on. The Monte Carlo technique describes the light propagation in the same way, as a random process consisting of one, two, …, N scattering events. The addition, in the theoretical description, of one more link of the ladder $\Lambda(R_{n\,n+1})p_0(\mathbf{k}_{n\,n+1} - \mathbf{k}_{n+1})$ is simulated, in the numerical experiment, by a path of a random length (characterized by the weight function) to the point of next collision. In the analytical theory, a chain of N scatterings corresponds to N coupling factors $\Lambda(R_{i\,i+1})$.

The complexity of the analytical calculation is that the integrals over $\mathbf{R}_i$ do not decouple because the phase functions depend on mutual positions of three scattering particles. The numerical simulation using the Monte Carlo technique decouples the chain by specifying a random value of the free path of the photon packet at each step. By virtue of the normalization condition for the phase function

$$\int p_0(\mathbf{k}_i - \mathbf{k}_s) d\Omega = 1 \quad (18)$$

the statistical weight of the photon packet after each scattering event remains the same.

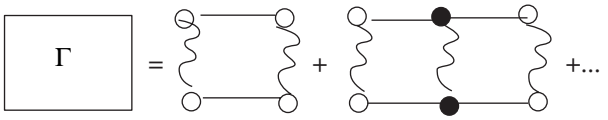


Fig. 2. A chain of ladder diagrams.

In the analytical approach, the conservation of the packet weight is due to the optical theorem. Indeed, $\int \Lambda(R) d\mathbf{R} = 4\pi l$ and, therefore, the expansion parameter of the iteration series (17) equals

$$\mu_s \int d\Omega_n \int d\mathbf{R}_{i+1} \Lambda(R_{i\,i+1}) p_0(\mathbf{k}_{i\,i+1} - \mathbf{k}) = \mu_s l. \quad (19)$$

In the absence of absorption ($l = l_s$), the quantity $\mu_s l$ exactly equals unity, which indicates conservation of the photon packet weight. In the analytical calculations, it is the condition $\mu_s l = 1$ that makes the successive approximation method unsuitable for solution of the Bethe–Salpeter equation.

The above comparison of the obtained analytical series (17) with the Monte Carlo technique makes it possible to generalize the latter to more interesting cases. Consider the problem of determination of the scattered light intensity taking into account the absorption ($\mu_a l \neq 0$). In this case, in each scattering event, the statistical weight of the photon packet decreases, in conformity with Eq. (19), by the factor

$$\mu_s l = (1 + l_s/l_a)^{-1}. \quad (20)$$

Thus, to take into account the absorption in the Monte Carlo technique, the weight of each photon packet should be multiplied by the factor (20). In this way, the intrinsic absorption can be taken into account exactly.

The calculation of the time correlation function differs from the calculation of the scattered light intensity only in that the weight of the photon packet, in the course of each scattering event, is multiplied by the phase function $p_t(\mathbf{k}_n - \mathbf{k}_{n-1})$.

In practice, most known applications [14, 15] deal with the diffusion mechanism of the time evolution of inhomogeneities, when the time correlation function of permittivity fluctuations may be represented in the form of the product of a statistical correlator and exponential function, i.e.,

$$G(q, t) \approx G(q, 0) \exp(-D_s q^2 t), \quad (21)$$

where D_s is the self-diffusion coefficient. When calculating the time correlation function in the form (21), it suffices to make the substitution

$$p_0(\mathbf{k}_n - \mathbf{k}_{n-1}) \longrightarrow p_0(\mathbf{k}_n - \mathbf{k}_{n-1}) \exp[-D_s(\mathbf{k}_n - \mathbf{k}_{n-1})^2 t]. \quad (22)$$

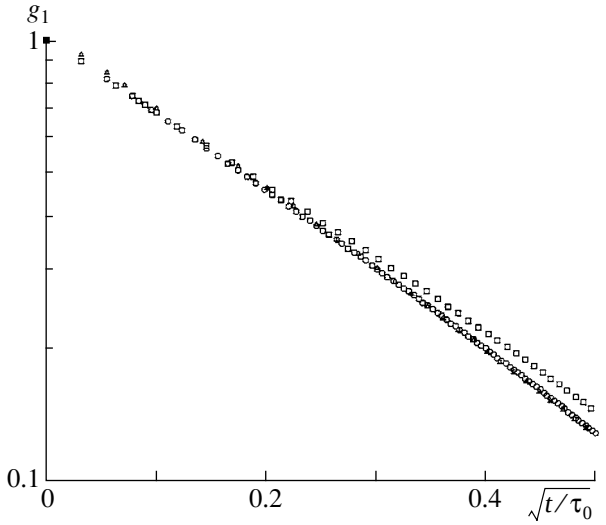


Fig. 3. The time correlation function of the field backscattered by a semi-infinite medium as a function of the argument $\sqrt{t/\tau}$ for three values of the anisotropy factor $g = \overline{\cos\theta}$: $g = 0$ (squares), $g = 0.5$ (circles), and $g = 0.9$ (triangles).

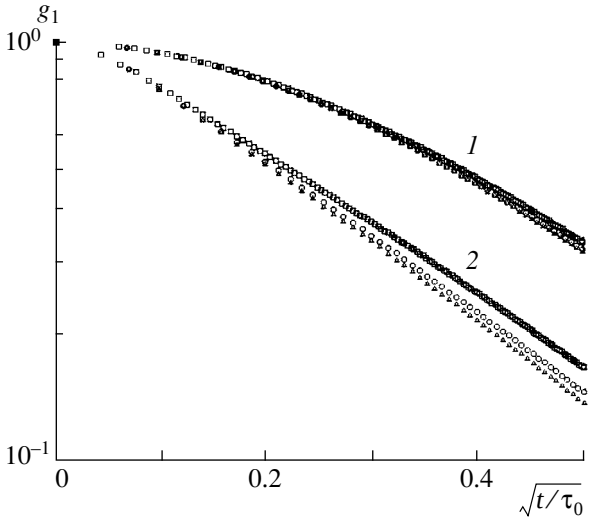


Fig. 4. The time correlation function of the field backscattered by a layer of finite thickness with $L = l^*$ (*1*) and $10l^*$ (*2*) for three values of the anisotropy factor: $\overline{\cos\theta} = 0$ (squares), 0.5 (circles), and 0.9 (triangles).

In the diffusion approximation, such a substitution is replaced by averaging of the momentum transfer,

$$D_s(\mathbf{k}_n - \mathbf{k}_{n-1})^2 t$$

$$\longrightarrow D_s\overline{(\mathbf{k}_n - \mathbf{k}_{n-1})^2} t = 2D_s k^2(1 - \overline{\cos\theta})t,$$

where $\overline{\cos\theta}$ is the average cosine of the scattering angle, which is the main parameter characterizing the anisotropy of the scattering indicatrix,

$$\overline{\cos\theta} = \int d\Omega_s p(\mathbf{k}_s - \mathbf{k}_i)\cos\theta_s / \int d\Omega_s p(\mathbf{k}_s - \mathbf{k}_i). \quad (23)$$

One can easily see that, in the case of a strong scattering anisotropy ($1 - \overline{\cos\theta} \ll 1$), the factor $2D_s k^2(1 - \overline{\cos\theta})t$ will be sufficiently small even for $t/\tau \sim 1$, where $\tau = 1/D_s k^2$ is the characteristic diffusion time of the scattering particle at a distance of the order of the wavelength.

According to Eq. (14), to simulate the peak of the coherent backscattering, one has to repeat the chain (12) in the same way as when calculating the scattered light intensity distribution, by specifying the direction from the source $\mathbf{k}_i$ and the direction to the detector $\mathbf{k}_s$. Note that, when calculating the detected signal, one has to exclude the cases of single scattering because they do not contribute to the cyclic diagrams. Finally, one has to perform summation over the positions $\mathbf{r}_D$ because the effect of coherent backscattering is observed only in the geometry of plane incoming and outgoing waves.

Consider the problem of simulation of the interference component of the backscattering. In the case of normal incidence and a small value of the backscattering angle θ_s, we may assume that $(\mathbf{k}_s + \mathbf{k}_i)/2 = \mathbf{k}_i$ and $\cos\theta_s \approx \cos\theta_i = 1$. According to Eq. (14), the entire difference from the expression for the intensity of the incoherent component consists in the presence of the factor $\exp[i\mathbf{q}_\perp(\boldsymbol{\rho}_1 - \boldsymbol{\rho}_2)]$. In view of the translational invariance with respect to the (x, y) coordinates along the plane interface (in the geometry of scattering from a plane layer), this factor may be substituted as follows:

$$\exp[i\mathbf{q}_\perp(\boldsymbol{\rho}_1 - \boldsymbol{\rho}_2)] \longrightarrow \cos(\mathbf{q}_\perp\boldsymbol{\rho}_{12}).$$

Thus, when separating out the intensity of the coherent component of the backscattering, one has to multiply the amount (or total weight) of the photon packets arriving at the interface with the wave vector $\mathbf{k}_s$ at a distance of ρ from the point of entrance by the factor $\cos(\mathbf{q}_\perp\boldsymbol{\rho})$ and to sum over the entire surface, i.e., over all values of ρ.

5. THE RESULTS OF SIMULATION

Figure 3 shows the results of simulation of the time correlation function of the field for three scattering media with different values of the anisotropy factor $\overline{\cos\theta} = 0$, 0.5, and 0.9. We have chosen the value $l = 3.3$ μm, which corresponds, for the given values of $\overline{\cos\theta}$, to the values of the transport length $l^* = 3.3$ μm for the isotropic case and 333 μm for the case of strong anisotropy ($\overline{\cos\theta} = 0.9$). In terms of $\sqrt{t/\tau}$, the time correlation function virtually does not depend on the single-scattering anisotropy. Note also a good agreement with experimental data [15]. The correlation func-

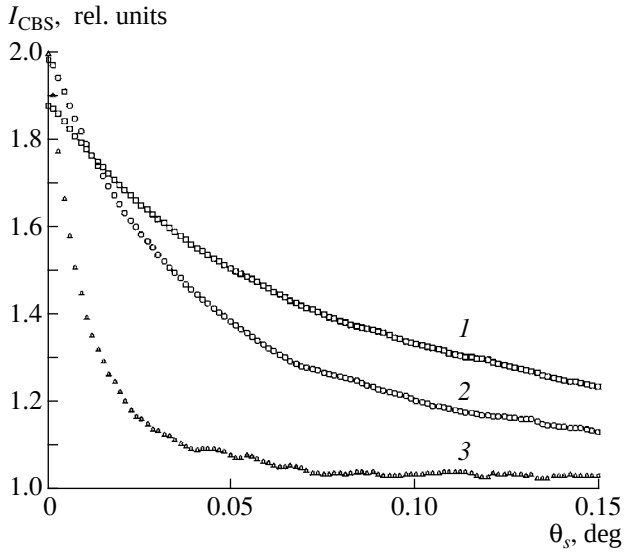


Fig. 5. The enhancement of the backscattering $B = 1 + I_{CBS}(\theta_s)/I(\theta_s)$ as a function of the angle θ_s. $I_{CBS}(\theta_s)$ is the intensity of the coherent backscattering, and $I(\theta_s)$ is the total intensity; the peak height in relative units equals 1.873 for $g = 0$ (*1*), 1.979 for $\overline{\cos\theta} = 0.5$ (*2*), and 1.995 for $g = 0.9$ (*3*).

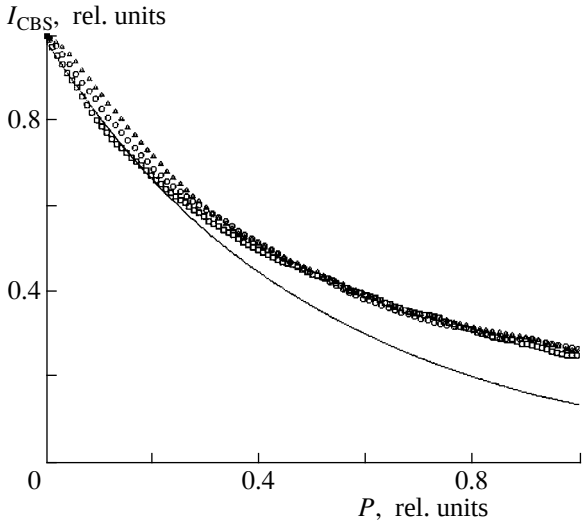


Fig. 6. The universal dependence of the coherent backscattering on the dimensional angular parameter $P = kl^*\sin\theta_s$. $\lambda = 0.6$ μm; $l = 33$ μm; and $\overline{\cos\theta} = 0$ (squares), 0.5 (circles), and 0.9 (triangles). The solid line is the approximation by $\exp(-2kl^*\sin\theta_s)$.

tion obtained can be well approximated by a formula of the type

$$g_1(t) \propto \exp(-\gamma\sqrt{6t/\tau}), \qquad (24)$$

proposed in the above paper.

Figure 4 shows the results of simulation of the time correlation functions of the field for layers of finite thickness with different values of the anisotropy factor. In this case, virtually all specific properties of the scattering system are seen to be also taken into account on passing to the description in units of the characteristic time τ. For the layer thickness $L \sim l^*$, the behavior of the correlation function, up to $t \sim 0.25\tau$, remains practically unaffected upon changes of the scattering anisotropy ($\overline{\cos\theta}$). For the layer $L = 10l^*$, the time correlation function decreases faster in the case of strong anisotropy. Note that the obtained dependences on the layer thickness L agree well with the predictions of the diffusion theory.

Figure 5 shows the results of calculation of the angular dependence of the coherent backscattering peak, also for the values $\overline{\cos\theta} = 0$, 0.5, and 0.9. Let $B = 1 + I_{CBS}(\theta_s = 0)/I(\theta_s = 0)$ be the parameter describing the enhancement of the backscattering. In our calculations, we obtained $B = 1.87$ for isotropic scattering, which agrees well with the value $B_{theor} = 1.88$ obtained in [16] on the basis of the generalized Milne solution. For $\overline{\cos\theta} = 0.9$, we obtained $B = 1.99$, which also agrees with the anticipated theoretical value $B = 2$ at $\overline{\cos\theta} \longrightarrow 1$. The dependence obtained for $\overline{\cos\theta} = 0.9$ is close to that obtained in [9]. The flat region appears to be slightly lower because the value of $l^* = 333$ μm is larger than the value of $l^* = 314$ μm used in [9].

As in the case of time correlations, the calculated angular dependence of the coherent backscattering peak, in terms of a dimensionless variable $\tilde{q} = kl^*\sin\theta_s$, appears to be universal (Fig. 6) and described sufficiently well by the formula $I_{CBS} \propto \exp(-\gamma kl^*\sin\theta_s)$ at $\gamma = 2$. Note that this dependence essentially differs from the dependence predicted by the diffusion approximation [17]

$$I_{CBS}^{dif} \propto 1 - 2\frac{(1+z^*)^2}{1+2z^*}kl^*\sin\theta_s,$$

at $kl^*\sin\theta_s \ll 1$, where $z^* = 0.71(1 - \overline{\cos\theta})^{-1}$. This formula yields the slope $\gamma^{dif} = 2.3$ at $\overline{\cos\theta} = 0$ and $\gamma^{dif} = 0.71$ at $\overline{\cos\theta} \longrightarrow 1$ [18]. Thus, in contrast to the diffusion approximation, which predicts a decrease in the linear slope factor of the coherent backscattering peak with increasing anisotropy, the dependence obtained in this paper indicates a universal nature of the decrease, virtually independent of the anisotropy.

6. CONCLUSIONS

We have shown the possibility of describing coherent effects within a united stochastic approach under the condition of multiple scattering. In simulating these effects, we used the Henyey–Greenstein phase function. Calculations of this kind may be performed, without difficulty, for suspensions, usually represented as

systems of rigid spheres [19–25]. The phase function in such a system is described as a product of the Mie form factor and the Percus–Yevick structure factor.

The analysis has shown that only for the calculation of intensity in a nonabsorbing semi-infinite medium is the scattering of a multiple nature. In all other cases, in the numerical method of calculation, the weight factor arising after each scattering event leads to a fast decay of the wave packet. In particular, to provide a multiple regime of radiation transfer, for an absorbing medium, the parameter $l_s/l_a \approx l/l_a$ should be small, and, for time-dependent functions with diffusion-type fluctuation decay, the parameter $D_s\overline{q^2}t = 2(t/\tau)(l/l^*)$ should be small. It is noteworthy, however, that, in the case of strong anisotropy of the phase function, the manifestations of coherent effects may turn out to be significant in spite of the smallness of these parameters. Indeed, the dependence of the intensity on absorption is controlled by the parameter l^*/l_a, which may be rather large compared with l/l_a. Similarly, the decay of the time correlations of the intensity is controlled by the parameter t/τ, which may substantially exceed the parameter $(t/\tau)(l/l^*)$. It is for exactly this reason that the correlation functions of intensity are described within the theory of multiple scattering even when they are reduced by two orders of magnitude.

A similar situation takes place for coherent backscattering. The trajectories simulated in the calculations of cyclic diagrams should involve a great number of scattering events if the parameter $kl\sin\theta_s$ (where θ_s is the backscattering angle) is small. Note that the decrease of the coherent backscattering peak is determined by the much larger parameter $kl^*\sin\theta_s$.

The comparative analysis performed in this paper makes it possible to significantly simplify simulation of radiation transfer and coherent effects in randomly inhomogeneous strongly scattering media, such as liquid crystals, biological tissues, etc., and to considerably widen the area of application of these methods.

ACKNOWLEDGMENTS

The work was supported by the Royal Society of London (grant no. 15298), the Russian Foundation for Basic Research (project no. 02-02-16577) and NATO (grant no. PST.CLG.979652). The authors are grateful to D.Yu. Churmakov for assistance in calculations and V.P. Romanov for valuable advice and comments in the process of preparation of the manuscript.

REFERENCES

1. V. P. Kandidov, Usp. Fiz. Nauk **166**, 1309 (1996) [Phys. Usp. **39**, 1243 (1996)].
2. M. Ospeck and S. Fraden, Phys. Rev. E **49**, 4578 (1994).
3. T. Iwai, H. Furukawa, and T. Asakura, Opt. Rev. **2**, 413 (1995).
4. K. Ishii, T. Iwai, and T. Asakura, Opt. Rev. **4**, 643 (1997).
5. S. E. Skipetrov and S. S. Chesnokov, Kvantovaya Élektron. (Moscow) **25**, 753 (1998).
6. R. Lenke and G. Maret, Eur. Phys. J. B **17**, 171 (2000).
7. R. Lenke and G. Maret, in *Scattering in Polymeric and Colloidal Systems*, Ed. by W. Brown and K. Mortensen (Gordon and Breach, London, 2000), pp. 1–73.
8. I. V. Meglinskiĭ and S. D. Matcher, Opt. Spektrosk. **91**, 692 (2001) [Opt. Spectrosc. **91**, 654 (2001)].
9. R. Lenke, R. Tweer, and G. Maret, J. Opt. A: Pure Appl. Opt. **4**, 293 (2002).
10. V. L. Kuz'min and V. P. Romanov, Usp. Fiz. Nauk **166**, 247 (1996) [Phys. Usp. **39**, 231 (1996)].
11. I. M. Sobol', *The Monte-Carlo Method* (Nauka, Moscow, 1985).
12. D. Y. Churmakov, I. V. Meglinski, and D. A. Greenhalgh, Phys. Med. Biol. **47**, 4271 (2002).
13. V. L. Kuzmin, V. P. Romanov, and L. A. Zubkov, Phys. Rep. **248**, 72 (1994).
14. D. J. Pine, D. A. Weitz, P. M. Chaikin, and E. Herbolzheimer, Phys. Rev. Lett. **60**, 1134 (1988).
15. G. Maret and P. Z. Wolf, Physica B (Amsterdam) **65**, 409 (1987).
16. M. C. W. van Rossum and Th. N. Nieuwenhuizen, Rev. Mod. Phys. **71**, 313 (1999).
17. E. Akkermans, P. E. Wolf, R. Maynard, and G. Maret, J. Phys. (Paris) **49**, 77 (1988).
18. F. C. McKintosh and S. John, Phys. Rev. B **40**, 2383 (1989).
19. M. H. Kao, A. G. Yodh, and D. J. Pine, Phys. Rev. Lett. **70**, 242 (1993).
20. Hu Gand, A. H. Krall, and D. A. Weitz, Phys. Rev. Lett. **73**, 3435 (1994).
21. P. D. Kaplan, A. D. Dinsmore, A. G. Yodh, and D. J. Pine, Phys. Rev. E **50**, 4827 (1994).
22. A. J. C. Ladd, Hu Gang, J. X. Zhu, and D. A. Weitz, Phys. Rev. E **52**, 6550 (1995).
23. K. Ishii, T. Iwai, and T. Asakura, J. Opt. Soc. Am. A **14**, 179 (1997).
24. V. V. Berdnik and V. A. Loiko, J. Quant. Spectrosc. Radiat. Transf. **63**, 369 (1999).
25. V. L. Kuz'min, V. P. Romanov, and I. V. Meglinskiĭ, Opt. Spektrosk. **96**, 139 (2004) [Opt. Spectrosc. **96**, 106 (2004)].



https://dspace.org/

Numerical simulation of coherent effects under multiple scattering of linearly polarized light.

Kuzmin, Vladimir L.; Meglinski, I. V.

2004-01-01T00:00:00Z
Springer Science Business Media
http://dspace.lib.cranfield.ac.uk/handle/1826/970
Optics and Spectroscopy (English translation of Optika i Spektroskopiya) Volume 97, Issue 1, 2005, Pages 100-106

Downloaded from a DSpace repository. https://dspace.org/